Hindawi
International Journal of Aerospace Engineering
Volume 2022, Article ID 4676944, 11 pages
https://doi.org/10.1155/2022/4676944

Research Article

Pretension Design and Analysis of Deployable Mesh Antenna considering the Effect of Gravity

Guanlong Su, Xiaofei Ma, Yang Li, Yesen Fan, and Hui Wang

Xi'an Institute of Space Radio Technology, Xi'an 710100, China

Correspondence should be addressed to Xiaofei Ma; maxf041600@sina.com

Received 17 March 2022; Revised 13 April 2022; Accepted 13 April 2022; Published 9 May 2022

Academic Editor: Tuanjie Li

The difference between the space and the earth environment has significantly influenced the shape accuracy of the antenna reflector surface. With the increasing demand for the aperture of the antenna reflector, gravity has become one of the main factors that restrict the accuracy. In this paper, a new method for pretension design considering the effect of gravity is proposed. The design surface can be well restored to the ideal surface in orbit. Meanwhile, this method can avoid flipping antenna reflectors or extensive experiments for modification during ground adjustment. Then, the feasibility and effectiveness of the design method are validated by several numerical simulations. Moreover, the results are compared with the previous method and the differences have been discussed in detail. Finally, the effects of cable radius, cable length, and elastic modulus of the mesh reflector have been researched, respectively.

1. Introduction

The deployable mesh antennas are widely used in spatial applications due to the good stowed/deployed ratio [1], such as TerreStar antenna, Skyterra antenna, AstroMesh hoop truss antenna, and the antenna of JAXA Engineering Test Satellite. With the vigorous development of aerospace technology, the demand for large-scale space deployable antennas is becoming urgent. At the same time, more requirements emerge in the aspects such as tiny signal transmission on the ground, great capacity of information transmission, and the realization of the high resolution of remote sensing. All of these lead to the necessity of a large aperture deployable antenna with high accuracy [2]. As an indispensable component that highly affects accuracy, the cable net structure is always one of the research hot pots. The cable net structure is a family of flexible tension structures characterized by geometric solid nonlinearities. The initial stiffness and shape can be achieved by pretension design. The purpose is to find a surface close to the desired surface under specific tension loads. Therefore, the pretension distribution plays a vital role in the surface accuracy of deployable mesh reflectors.

To form a parabolic surface, the rigidity of deployable mesh reflectors is supplied by applying pretension to the cables. This process of pretension design is called form-finding [3]. Several traditional form-finding methods have been developed, such as force density, dynamic relaxation, inverse iteration, and genetic. The force density method was the most widely used and was introduced by Schek [4].

It first transforms the nonlinear equilibrium equations into linear ones with the concept of "force density." Then, the equilibrium equations are solved by numerical method to obtain the equilibrium pretension. Then, several methods have been carried out that only consider the cable net structure as in [5, 6]. Deng et al. improved the pretension design method and considered the multiple uncertainties [7–9]. Shi et al. proposed methodologies to automatically generate pseudogeodesic mesh geometries of spherical and parabolic reflector surfaces [10, 11]. The truss is treated as rigid in [12–17] when considering the rim truss. Yang et al. [18, 19] considered the elastic rim trusses and proposed an optimal method. Nie et al. also considered the flexible frames and proposed an integrated form-finding method [20–23]. Thermal effects have also been discussed. Shi et al. proposed a new methodology of mesh geometry design [24]. Tabata

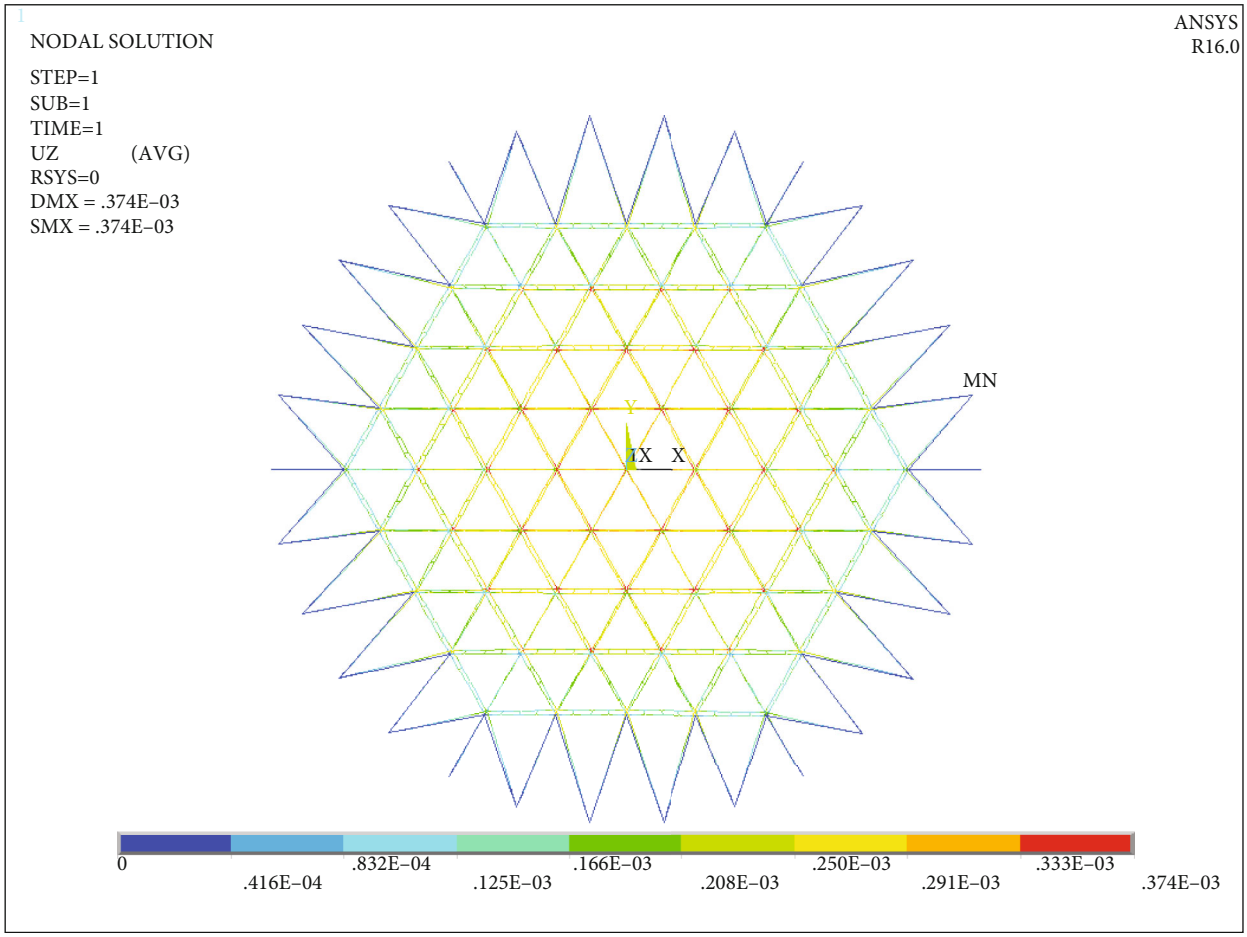

Figure 1: Nodal displacement calculated by ANSYS: subdivided finite element model.

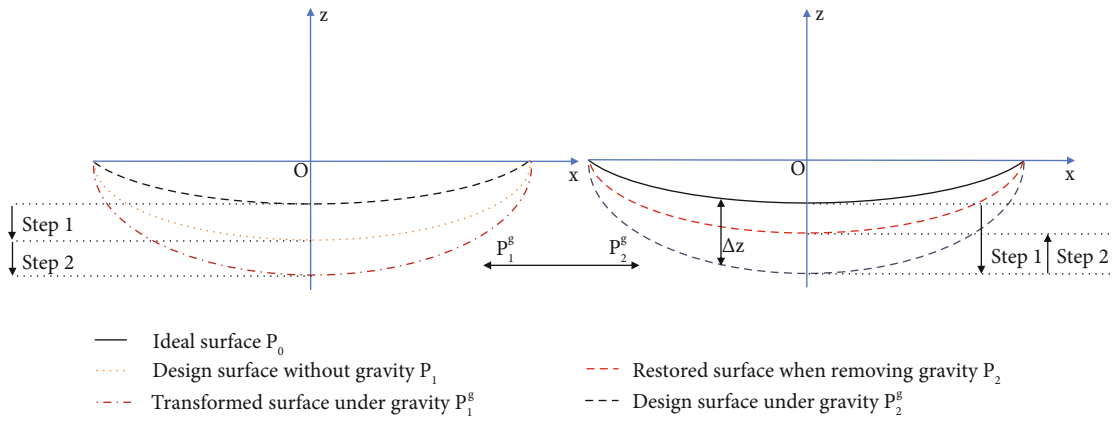

Figure 2: The comparison between two pretension design methods. (a) General method. (b) Method in this paper. The deviation between P_1^g and P_2^g increases as the antenna aperture increases.

and Natori had explored shape control concepts for mesh reflectors [25–29].

However, these existing methods are only suitable in an ideal environment. That means no gravity effect is taken into consideration. An accurate antenna reflector should be adjusted on the ground where gravity cannot be ignored. Moreover, the influence of surface accuracy resulted by gravity increases as the size of the antenna increases. Two methods are widely used in engineering to estimate the effect of gravity. The first is to flip the antenna reflector to get cup-up and cup-down surfaces by adding the two together to counteract the effect of gravity [30, 31]. This method requires a sizeable

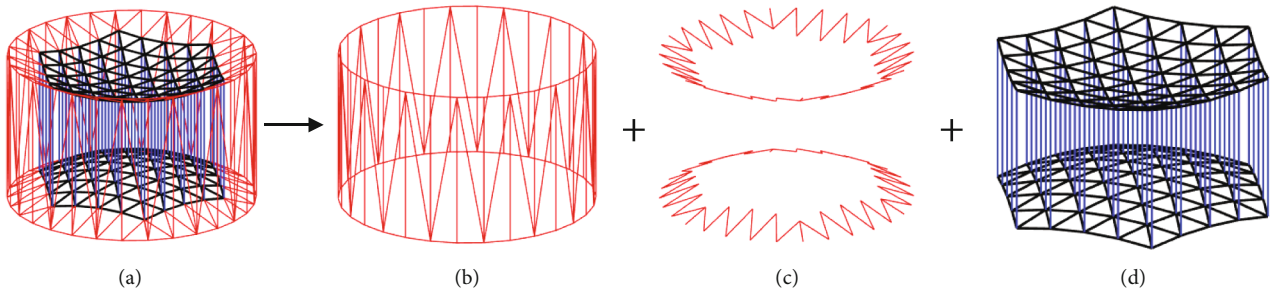

Figure 3: Composition of a mesh reflector. (a) Mesh reflector. (b) Truss. (c) Boundary cable. (d) Cable net.

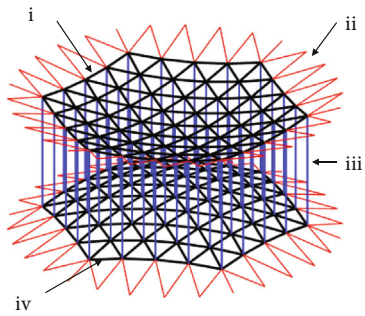

Figure 4: Schematic of a cable net structure. (a) Front cable net. (b) Boundary cables. (c) Tension tie cables. (d) Back cable net.

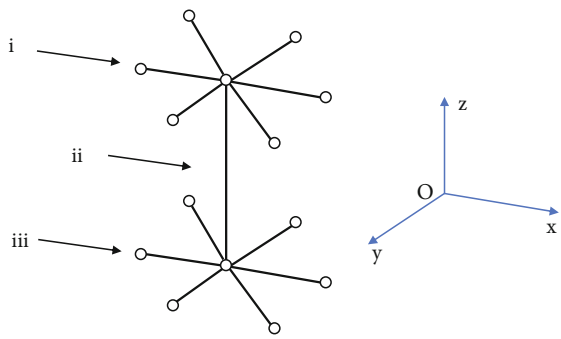

Figure 5: A cable net unit. (a) Front cable net. (b) Tension tie cable. (c) Back cable net.

experimental site and adjusting work is extremely difficult. As the antenna diameter increases, it has a significant risk to flip the antenna. Considering that the mesh antenna is a large flexible structure, flipping may cause other assembly errors or damage the antenna. The second one is based on finite element software. This method needs to combine the experimental results with the error correction method [32–34]. The critical factor is to give static loads in the form of distributed weights to the nodes of the cable net and measure the surface deformation caused by the static loads. Then, adjust the stiffness parameters to make the deformation characteristics of the mathematical model exactly match the test results. However, there are thousands of positions where static loads should be applied when the antenna aperture is large, which makes this method extremely difficult to apply in practice. Not only is there a large number of experiments, but the matching of mathematical models and experimental results is also difficult to achieve at this magnitude.

Specifically, the mesh surface is first designed according to the ideal one. Then, the deformed surface under gravity is obtained by finite element simulation. Introducing gravity into the finite element model to get the reference surface in the stage of ground adjustment is acceptable in a certain aperture range. This can be seen in Figure 1. However, when the aperture further increases, there is an obvious deviation as discussed in 4.3. Generally, model modification is necessary when considering manufacture based on the methods mentioned above. There both have insurmountable problems in the stage of ground adjustment when the aperture increases. To solve this problem, the gravity factor should be introduced in the pretension design process first. At the same time, the change of cable stiffness should also be considered in the design. There are two critical problems in this issue. The first is that the target shape of the design is no longer an ideal shape but an unknown gravitational surface. The second is whether the surface can meet the surface accuracy requirements after the gravity is removed.

The primary purpose of this paper is to propose a new method to design the pretension in the cable net structure. A new model considering gravity can be achieved to supply guidance in antenna adjustment. Generally, the pretension design considering gravity is shown in Figure 2(a), and the method in this paper is shown in Figure 2(b). The comparison of the two design methods has been discussed in detail in 3.3. The biggest difference is that the method in this paper is designed with changes in gravity and stiffness. Furthermore, the advantage of the method in this paper is that it does not require flipping the antenna or extensive experimental corrections. It should be noted that although the designed surface considering gravity can effectively guide the ground adjustment, the surface must be restored to meet the accuracy requirements after entering the orbit. This point is the most critical condition for design convergence, consistent with previous studies.

2. Composition of a Mesh Reflector

A deployed mesh reflector antenna is conceived with the concept of a tension truss, which is a light and inherently stiff structure that can be precisely and repeatedly deployed regardless of the environment. As illustrated in Figures 3 and 4, it is divided into three parts, a supporting truss, a

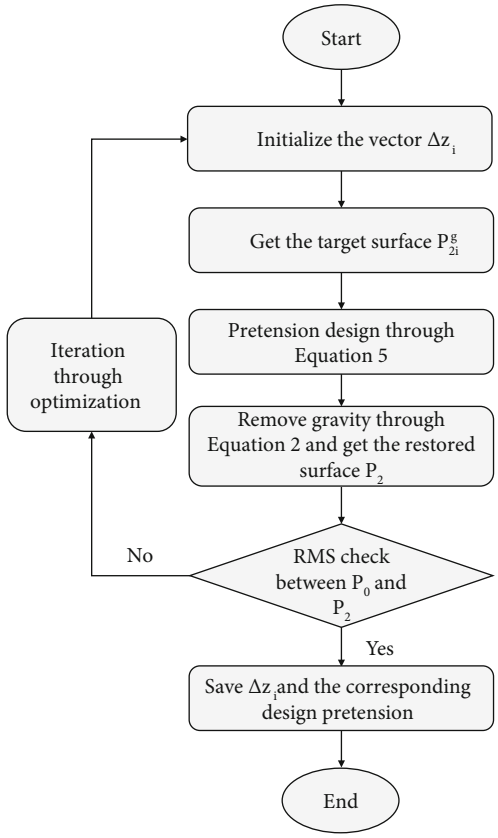

Figure 6: Algorithm of pretension optimization.

boundary cable, and a cable net reflector, including surface cables, tension tie cables, and RF reflective mesh which are sewn on the net surface. The cable net reflector and the boundary cables are named the deployable cable net structure.

3. Pretension Design Method

3.1. Mechanical Analysis of Cable. The space environment is known as a microgravity environment. Therefore, the straight-rod elements can achieve calculation accuracy that meets high efficiency in engineering requirements. According to the principle of virtual displacement, the overall stiffness matrix considering the pretensioned cable element can be divided into two parts when omitting the second-order term. They are k_E and k_G that represent the elastic stiffness matrix and geometric stiffness matrix, respectively. For a cable element in the local coordinate system, the coordinates of both ends are $(0, 0, 0)$ and $(x_j, 0, 0)$. Then, the relationship between nodal displacement and nodal force can be shown in

$$\begin{aligned} [k_E + k_G]d &= f - r, \\ r &= A_c l_c A^T \sigma - f, \\ k_E &= A_c l_c E_c \left[A^T A\right], \\ k_G &= A_c l_c \left[\sigma B^T B\right], \end{aligned} \tag{1}$$

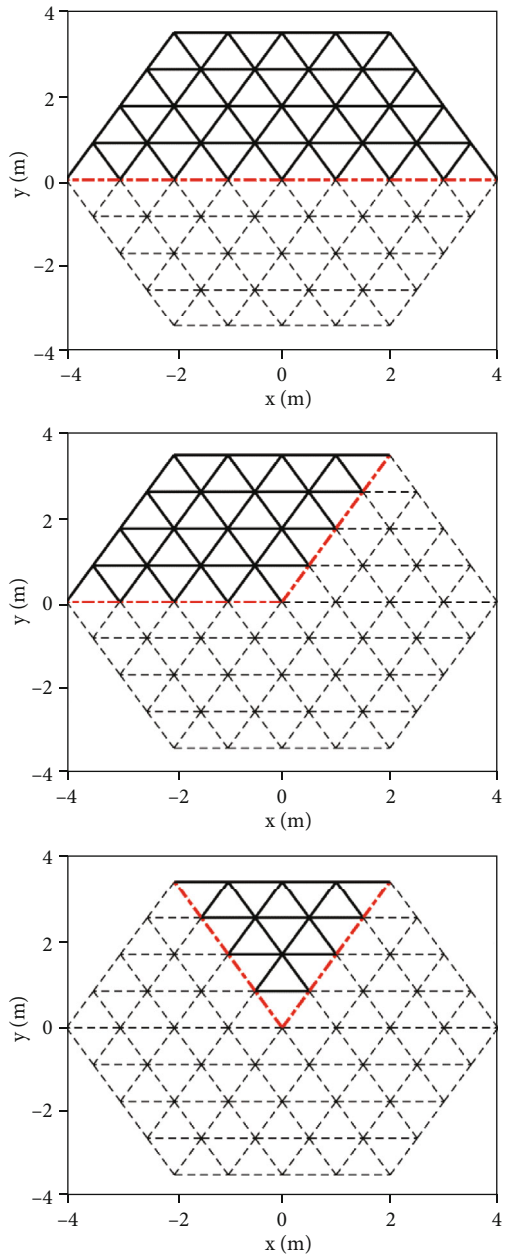

Figure 7: Characteristic structure of cable net.

where

$$\begin{aligned} A &= (b_1\, 0\, 0\, b_2\, 0\, 0), \\ B &= \begin{pmatrix} b_1 & 0 & 0 & b_2 & 0 & 0 \\ 0 & b_1 & 0 & 0 & b_2 & 0 \\ 0 & 0 & b_1 & 0 & 0 & b_2 \end{pmatrix}, \\ b_1 &= -b_2 = -\frac{1}{x_j}. \end{aligned} \tag{2}$$

And E_c, l_c, A_c, σ, f, and d indicate the elastic modulus, cable length, cross-sectional area, cable stress, external force, and nodal displacement. Then, in the overall coordinate

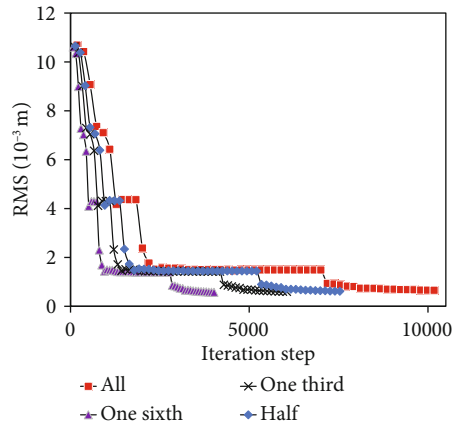

Figure 8: Iteration process of RMS error of the front cable net (interior point algorithm).

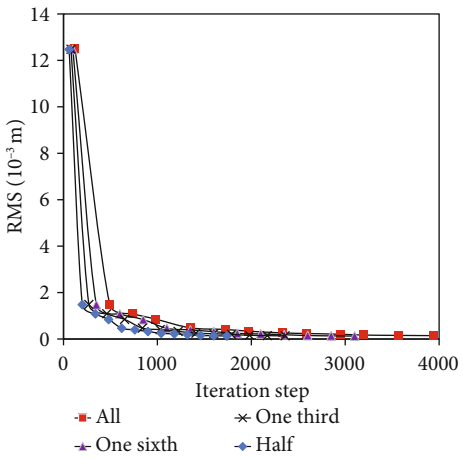

Figure 9: Iteration process of RMS error of the front cable net (quasi-Newton algorithm).

system, the above equation can be transformed by the transformation matrix to obtain the stiffness equation of the cable element.

$$[K_E + K_G]D = F - R. \tag{3}$$

By assembling the stiffness matrix equations of each cable element in the global coordinate system, the overall stiffness equation of the entire cable net structure can be obtained. When the pretensions have been designed and the external force is specific, the overall deformation of the cable net can be obtained through the stiffness equation.

3.2. Effect of Gravity. The pretension design of a cable net structure aims to determine the cable tension distribution to obtain the required reflector surface accuracy. The unit of a cable net structure is shown in Figure 5, where node i is connected to node j by a cable. The equilibrium equation of node i can be derived as follows.

$$\begin{cases} \sum_j F_{ij} \dfrac{x_i - x_j}{l_{ij}} = 0, \\ \sum_j F_{ij} \dfrac{y_i - y_j}{l_{ij}} = 0, \\ \sum_j F_{ij} \dfrac{z_i - z_j}{l_{ij}} = \sum_j G_{ij}, \end{cases} \tag{4}$$

where F_{ij}, G_{ij}, and l_{ij}, respectively, represent the tension force, the gravity, and the length of the cable between two adjacent nodes i and j of coordinates (x_i, y_i, z_i) and (x_j, y_j, z_j). It can be rewritten in the form of a matrix as follows:

$$Q_{3k\times r} F = C, \tag{5}$$

where $C = \begin{pmatrix} 0_{2k\times 1} \\ G_{k\times 1} \end{pmatrix}$.

Q is a coefficient matrix; $F = (\, F_1 \quad F_2 \quad \cdots \quad F_r \,)^T$ is the tension force vector of cables; k is the total number of free nodes; r is the total number of cables.

Since the assumption of nodes located in the required parabolic surface, the nodal locations and topology of the cable net structure can be determined. Then, the pretension design of the cable net structure can be expressed by the following optimization model:

$$\begin{cases} \text{Find} \quad F = (\, F_1 \quad F_2 \quad \cdots \quad F_r \,)^T, \\ \text{Min} \quad \text{RMS} = \sqrt{\dfrac{\sum_{j=1}^{n} \Delta S_j^2}{n}}, \\ \text{s.t.} \quad Q_{3k\times r} F = C, \\ \qquad F_i > 0 \qquad\qquad 1 \le i \le r, \end{cases} \tag{6}$$

where ΔS_j is the displacement of the jth free node in the cable net reflector, n is the total number of free nodes in the cable net reflector, and RMS is an abbreviation of the root mean square.

It should be noticed that the length of the cable changes in each iteration step after being pretensioned. In such cases, the gravity matrix also changes in each step. However, the original lengths of all cables before being pretensioned are considered unchanged.

3.3. Optimization Design Method. For a given antenna surface, the pretension can be designed through Equation (6) considering the effect of gravity. Nevertheless, the target position of the antenna reflector is unknown. Specifically, when gravity is not taken into consideration, the design surface is simply the ideal surface P_0 in orbit. However, the design surface under gravity would be deformed to P_2^g, which means that the target surface is unknown during the optimization. The difference can be illustrated in Figure 2. As gravity only works in z direction, the influences of the

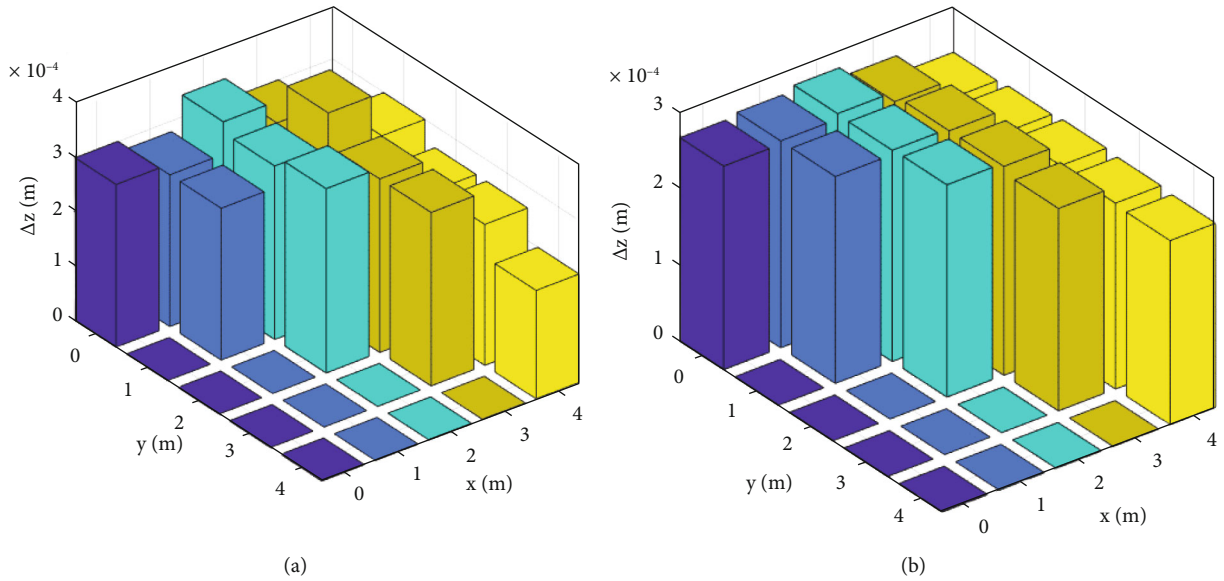

Figure 10: Surface error of front cable net considering the effect of gravity. (a) Optimization results. (b) Finite element calculation results.

coordinates in the x and y directions are ignored. There is a deviation Δz, which is unknown, between the target surface under gravity and the ideal surface. But for every certain value of Δz_i, pretension can be designed for the ith target surface. Moreover, this undergravity surface should have the ability to restore to an ideal position on orbit as required. Gravity is removed through Equation (3) after the design so that the surface would deform to a new position P_2 as shown in Figure 2. The smaller the gap between P_0 and P_2, the better it is. Obviously, all values of Δz for free nodes are negative and for boundary nodes the values are 0. The solution is to find a certain Δz with which pretension design can be solved. Then, the surface is able to recover to the ideal surface after removing the gravity. The overall algorithm is presented in the flowchart of Figure 6.

The selection of the initial values of the iteration is a critical factor in the optimization. An improper selection of the initial value will cause the result to be a local optimum instead of a global optimum. And the iteration may not converge in worst cases. To solve this problem, the values are selected by the combination of the engineering experience and the calculation results.

3.4. Improvement of Optimization. According to the above discussion, in the mathematical model of the cable net structure, each value of Δz_i is an optimization variable. In this case, even if we optimize the mathematical model to the maximum, the number of variables is still large. Taking an antenna with a diameter of 10 m as an example, the node number is 182, within the allowable range of the geometric size of the cable network. The optimization problem of this dimension not only requires a lot of computing time but also is prone to nonconvergence. Here, we need a more efficient method to reduce the number of optimization variables while ensuring the accuracy.

Fortunately, the cable net structure is a highly symmetric structure, which allows us to simplify it in different ways. According to the symmetrical form, half, one-third, and one-sixth of the cable net can be taken as a characteristic structure, as shown in Figure 7. However, the boundary of the characteristic structure is different from the original cable net. If we only use the characteristic structure for optimization, the cable stress of the nodes at the position of the red line in Figure 7 will change. When the calculation result of the characteristic structure is substituted into the cable net, there will be inevitable deformation. Although this deformation can be estimated, it will affect the stability of the optimization. The calculation time will be longer and even fail to converge, which is contrary to our original intention. In this case, we should still optimize with variables of the same dimension, but the total number of variables is reduced. That is to say, half, one-third, and one-sixth of the number of variables are used, respectively, and then, other nodes are valued according to the symmetrical relationship. Taking an antenna with a diameter of 10 m as an example, we now only set 102, 78, and 42 variables in the case of half, one-third, and one-sixth, respectively. Then, other values of Δz_i can be settled, and the dimension of Δz will still be 182. By this method, we can reduce the number of variables and do not change the boundary conditions of the cable network.

4. Results and Discussion

4.1. Pretension Design of a 10 m Mesh Reflector. A parabolic antenna with a spatial mesh reflector is shown in Figure 4. The antenna specifications are as follows:

Diameter of aperture: 10 m
Focal length of front cable net: 7.5 m
Focal length of back cable net: 7.5 m
Number of surface cables: 312 (= 156 × 2)
Number of boundary cables: 108 (= 54 × 2)
Number of tension tie cables: 61
Number of free nodes: 122 (= 61 × 2)

Table 1: Pretension distribution of the cable net.

Item	Pretension values in cables (N)		
	Maximum	Minimum	Mean
Front cable net	48.61	44.56	45.76
Back cable net	48.72	44.48	45.77
Tension tie cables	10.61	8.92	9.48

Table 2: Pretension distribution of the cable net with different aperture diameters.

Diameter of aperture (m)	Item	Pretension values in cables (N)		
		Maximum	Minimum	Mean
10	Front cable net	84.20	50.52	69.12
	Back cable net	47.56	28.04	33.52
	Tension tie cables	10.48	7.52	9.40
12	Front cable net	85.36	48.67	70.12
	Back cable net	47.12	27.44	32.48
	Tension tie cables	10.34	7.36	9.25
16	Front cable net	86.88	47.64	68.84
	Back cable net	46.88	25.44	31.92
	Tension tie cables	10.28	7.28	9.16
20	Front cable net	88.94	48.36	70.34
	Back cable net	45.24	21.68	28.48
	Tension tie cables	12.36	6.28	8.83
24	Front cable net	92.34	53.08	72.56
	Back cable net	42.76	21.56	27.44
	Tension tie cables	11.24	5.84	8.72

Height: 2 m
Type of facets: triangular
Elastic modulus of cables: 20 GPa
Radius of cables: 0.5×10^{-3} m
Density of cables: 1450 kg/m^3

First, it is important to set the initial value of Δz, which can be expressed as

$$\Delta z = \left[\Delta z_1, \Delta z_2, \cdots, \Delta z_{n_f}, \underbrace{0, 0, \cdots 0}_{n_b}\right], \quad (7)$$

where n_f and n_b represent the number of free nodes and boundary nodes, respectively. This model is simulated in different ways. Corresponding to 3.4, all free nodes, half of the free nodes, one-third of the free nodes, and one-sixth of the free nodes are used as optimization variables, respectively. All values of Δz is constrained to be negative. The tension forces of all cables are set to 40 N initially. Constrained nonlinear minimization is used to solve the problem. The iteration results of interior point algorithm and quasi-Newton algorithm are shown in Figures 8 and 9, respectively.

When using interior point algorithm, the RMS error between P_0 and P_2 of front cable net is lowered from 11.07 $\times 10^{-3}$ m to 0.66×10^{-3} m. When all free nodes are used as optimization variables, the integration step is 10711. When the characteristic structure is used to reduce the optimization variables, the integration steps are significantly reduced and the optimization results remain consistent. The results show that this method is scientific and necessary when the aperture increases.

Meanwhile, when the quasi-Newton algorithm is used, the RMS error between and of the front cable net is lowered from 12.49×10^{-3} m to 0.14×10^{-3} m. The integration step is 3936 which is much smaller than the first algorithm. The optimization result is better at the same time. Likewise, with the introduction of characteristic structures, the efficiency of optimization computations continues to increase. It can be seen from the comparison that although there are many optimization variables, the optimization results are completely acceptable in engineering. This is due to the highly symmetrical feature of the cable net structure. On the other hand, the choice of algorithm and the initial value is critical, affecting the optimization efficiency and effectively avoiding nonconvergence when the antenna aperture is continuously increased.

The surface of the front cable net considering the effect of gravity is shown in Figure 10. Only one-sixth of the model is shown in this figure. All values are negative and are taken as absolute values in the figure. The maximum nodal displacement of Δz is -0.34×10^{-3} m. Compared with the finite element calculation results, each value of Δz in the optimization results has a degree of discrimination, and the finite element calculation results are close to the same. However, the difference between the overall results is small, which shows that there is little difference between the two methods when the diameter is 10 m. The pretension distribution of the cable net structure is shown in Table 1. The design surface is basically in line with the prediction, which confirms the validity of pretension optimization. On the other hand, the forces in Table 1 show excellent uniformity that indicates a good stability in the design results. The maximum and minimum stress ratios of the front cable net and the back cable net are 1.062 and 1.096, respectively. More importantly, the surface we find has the ability to restore to the ideal surface when removing gravity. The minimum RMS between two surfaces is only 0.14×10^{-3} m which is acceptable in engineering.

In order to verify the accuracy of the calculation, a subdivided finite element model is established and distributed

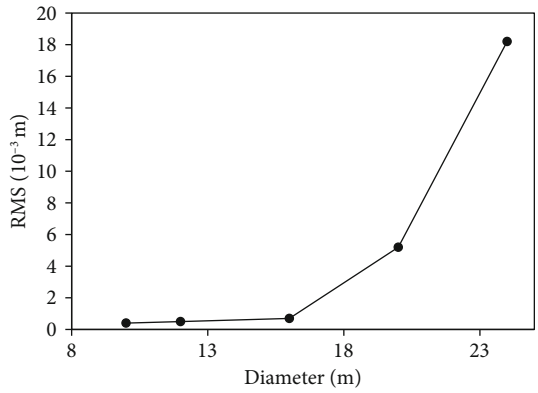

Figure 11: Deviation between P_1^g and P_2^g.

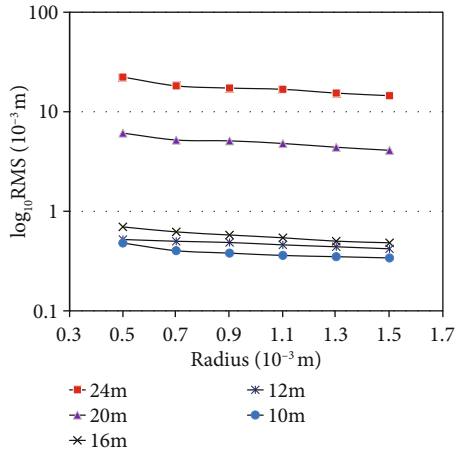

Figure 12: Effect of the cable radius.

gravity is applied on the model. In the subdivision model, multisegment elements are used to simulate the catenary cable. The subdivided model is verified by ANSYS as shown in Figure 1 in the manuscript. The maximum nodal deviation caused by gravity between the subdivided model and theoretical method in this paper is $0.37 \times 10^{-3} - 0.28 \times 10^{-3} = 0.09 \times 10^{-3}$ m, which meets the requirement (less than 0.1×10^{-3} m at least).

4.2. Pretension Design with Reflective Mesh. Taking into account the needs of large-aperture antennas in engineering applications, the algorithm is used to simulate antennas of different apertures with the influence of RF reflective mesh ($5 \times 10 - 2\,\text{kg/m}^3$), and the results are shown in Table 2.

This method can still effectively carry out the pretensioning design when considering the reflective metal mesh. The optimization method has specific stability when the antenna aperture is continuously increased. There is no failure to converge. When only considering the cable mesh structure, the pretension values of the front and back cable meshes are the same. However, after considering the RF reflective mesh, the stress on the front mesh surface increases significantly, resulting from the gravity of the RF reflective mesh directly acting on the front mesh surface. At the same time, the uniformity of pretension decreases clearly, which is closely related to the boundary of the cable net structure. On the other hand, although the pretension values of the tension cable and the back net do not change much, they also become nonuniform.

4.3. Deviation between P_1^g and P_2^g. Generally, the ideal shape P_0 is taken as the target shape during the pretension design of the antenna reflection surface. And some methods are used to iteratively calculate it to accomplish the pretension design and form-finding work. The shape obtained at this time can be called P_1, and the validity of the design is verified by comparing the RMS value of P_1 and P_0. When considering the effect of gravity, a gravity load is applied to P_1 surface to obtain P_1^g. In fact, this method is not accurate enough due to simplification. Here, the designed surface in ideal condition under gravity P_1^g and the designed surface considering gravity P_2^g are compared. It can be seen in Figure 11 that when the antenna diameter is between 10 m and 16 m, the RMS deviation of the two surfaces is minimal, only increasing from 0.402×10^{-3} m to 0.697×10^{-3} m. However, when the aperture is further increased, the deviation of the two surfaces increases sharply, and the deviation has reached 18.2×10^{-3} m when the diameter is 24 m. This also confirms that it is impossible to obtain an accurate ground surface only by loading the gravity on the design surface that does not consider gravity. This is also why the surface cannot be directly used to complete the ground adjustment in engineering. At the same time, the deviation of the two surfaces is in the form of the exponential distribution, which is related to the structure and stiffness of the cable net. When the diameter of the antenna is small, gravity is not a significant factor, but when the diameter of the antenna increases continuously, the gravity has a significant influence on the precision of the pretension and the surface.

4.4. Effect of Cable Radius. From the previous discussion, it can be concluded that when the antenna aperture is large, there is a big difference between whether gravity is considered in the pretension design stage. A natural question as whether this is caused by other factors arises. The antenna reflector mainly comprises cables, so the cable length, cable radius, and elastic modulus are all critical parameters. Firstly, the research is carried out with the radius of the cable as a variable, as shown in Figure 12.

It can be seen from the figure that when the cable radius changes, the overall RMS value shows a downward trend. When the cable radius increases, the gravity of the cable net structure increases, but the gravity of the RF reflective mesh does not change. It can be concluded that when the stiffness of the cable net structure increases, the effect of coupling with the RF reflective mesh will be weakened. However, this weakening does not make the two surfaces P_1^g and P_2^g consistent. That is to say, when the diameter of the antenna is large, changing the radius of the cable slightly impacts the surface accuracy. This may be because the gravity of the RF reflective mesh far exceeds that of the cable mesh.

4.5. Effect of Cable Length. The cable length in the cable net structure directly determines the fineness of the

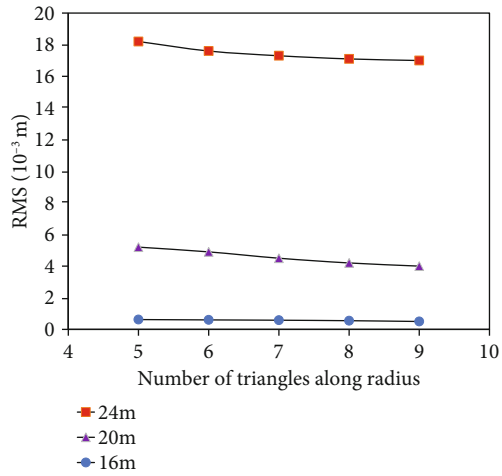

Figure 13: Effect of the cable length.

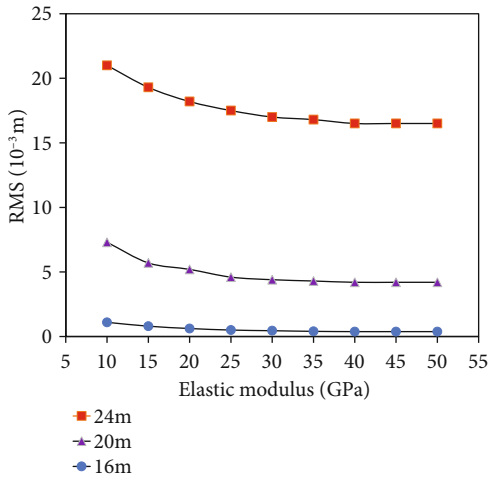

Figure 14: Effect of the elastic modulus.

mathematical model. The smaller the cable length, the more triangle segments along the radial direction. To make antennas of different diameters comparable, the number of segments in the radius triangle is used as an independent variable, and the number of segments is inversely proportional to the length of the cable. The results are shown in Figure 13. The RMS value decreases with the decrease of the cable length. Thanks to the refinement of the model, which leads to the smaller calculation error. However, generally the values tend to be stable within a certain range. This shows that the deviation between the surfaces P_1^g and P_2^g is not due to geometric errors. It also shows that when the diameter of the antenna is large, gravity greatly influences the surface accuracy.

4.6. Effect of Elastic Modulus. The elastic modulus of the cable directly affects the stiffness. When the elastic modulus increases, the effect of gravity becomes smaller and smaller. The data in Figure 14 illustrate the same conclusion. However, as the elastic modulus increases to a specific value, the value of RMS no longer decreases but tends to remain unchanged. This also shows that the two surfaces P_1^g and P_2^g are different. That implies the necessity to consider gravity in the pretension design.

5. Conclusions

A novel pretension design method considering the effect of gravity is proposed. Compared with previous methods, it can avoid flipping the antenna or excessive experiments in the stage of ground adjustment in engineering. At the same time, the method can ensure that the antenna can restore to the surface that meets the accuracy requirements after entering the orbit. Furthermore, with the increase of the antenna aperture, the method shows specific stability and does not fail to converge.

Considering that there are too many optimization variables in this optimization method, the characteristic structure is selected according to the symmetry of the cable net structure. Although the dimensions of the variables in the iterations remain unchanged, reducing the variables still effectively reduces the number of iterations. Two algorithms are used for the calculation, and the results show that the initial values according to engineering experience and calculation results are valid in the optimization.

Numerical simulations of cable net antennas with diameters ranging from 10 m to 24 m are carried out. After introducing the gravity of the RF reflective mesh, an excellent pretension distribution can still be obtained. Two surfaces are compared. When the antenna diameter is not large, the difference between the two is minimal. As the antenna aperture increases, the RMS values of the two increase exponentially. Then, the effects of cable radius, length, and elastic modulus are analysed. When the cable radius increases, the deviation of the two surfaces will decrease slightly. The same phenomenon occurs when the elastic modulus increases. However, the deviation tends to remain unchanged when the elastic modulus increases to a certain extent. When the length of the cable is changed, which will refine the model, the deviation of the two surfaces will decrease but always remain within a specific range.

In general, when the diameter of the antenna increases, the influence of gravity becomes increasingly significant. Therefore, the method proposed here can effectively estimate the ground surface of the antenna. At the same time, the flipping and experimental correction of the antenna are avoided. This is of great significance to surface adjustment in engineering. In future work, the comparison of experimental data is needed to verify the proposed method's effectiveness better.

Data Availability

The data used to support the findings of this study are available from the first author upon request.

Conflicts of Interest

The authors declare that there is no conflict of interest regarding the publication of this paper.

Acknowledgments

This work is supported by previous research in the 20th International Symposium on Distributed Computing and Applications for Business, Engineering and Science [35]. We thank all the authors for their research.

References

[1] T. J. Li, "Deployment analysis and control of deployable space antenna," *Aerospace Science and Technology*, vol. 18, no. 1, pp. 42–47, 2012.

[2] X. F. Ma, Y. P. Song, and T. J. Li, "Mesh reflector antennas: form finding analysis review," in *54th AIAA/ASME/ASCE/AHS/ASC Structures, Structural Dynamics and Materials Conference*, Boston, Massachusetts, 2013.

[3] T. J. Li, J. Jiang, H. Q. Deng, Z. C. Lin, and Z. W. Wang, "Form-finding methods for deployable mesh reflector antennas," *Chinese Journal of Aeronautics*, vol. 26, no. 5, pp. 1276–1282, 2013.

[4] H. J. Schek, "The force density method for form finding and computation of general networks," *Computer Methods in Applied Mechanics and Engineering*, vol. 3, no. 1, pp. 115–134, 1974.

[5] A. G. Tibert, "Optimal design of tension truss antennas," in *44th AIAA/ASME/ASCE/AHS/ASC structures, structural dynamics and materials conference*, Norfolk, Virginia, 2003.

[6] B. Yang, H. Shi, M. Thomson, and H. Fang, "Optimal design of initial surface profile of deployable mesh reflectors via static modeling and quadratic programming," in *50th AIAA/ASME/ASCE/AHS/ASC structures, structural dynamics and materials conference*, Palm Springs, California, 2009.

[7] H. Q. Deng, T. J. Li, and Z. W. Wang, "Design of geodesic cable net for space deployable mesh reflectors," *Acta Astronautica*, vol. 119, pp. 13–21, 2016.

[8] H. Q. Deng, T. J. Li, Z. W. Wang, and X. Ma, "Pretension design of space mesh reflector antennas based on projection principle," *Jounral of Aerospace Engineering*, vol. 28, no. 6, article 04014142, 2015.

[9] H. Q. Deng, T. J. Li, and Z. W. Wang, "Pretension design for space deployable mesh reflectors under multi-uncertainty," *Acta Astronautica*, vol. 115, pp. 270–276, 2015.

[10] H. Shi, B. Yang, and H. Fang, "Offset-feed surface mesh generation for design of space deployable mesh reflectors," in *54th AIAA/ASME/ASCE/AHS/ASC Structures, Structural Dynamics, and Materials Conference*, Boston, Massachusetts, 2013.

[11] H. Shi, B. Yang, M. Thomson, and H. Fang, "Automatic surface mesh generation fordesign of space deployable mesh reflectors," in *53rd AIAA/ASME/ASCE/AHS/ASC Structures, Structural Dynamics, and Materials Conference*, Honolulu, Hawaii, 2012.

[12] G. Yang, D. Yang, Y. Zhang, and J. Duand, "Form-finding design of cable-mesh reflector antennas with minimal length configuration," *Aerospace Science and Technology*, vol. 63, pp. 9–17, 2017.

[13] D. Yang, G. Yang, Y. Zhang, and J. Du, "Least-squares minimization of boundary cable tension ratios for mesh reflectors," *AIAA Journal*, vol. 56, no. 2, pp. 883–888, 2018.

[14] W. Liu and D. Li, "Simple technique for form-finding and tension determining of cable-network antenna reflectors," *Journal of Spacecraft and Rockets*, vol. 50, no. 2, pp. 479–481, 2013.

[15] Y. Tang, T. Li, X. Ma, and L. Hao, "Extended nonlinear force density method for form-finding of cable-membrane structures," *Journal of Aerospace Engineering*, vol. 30, no. 3, article 04016101, 2017.

[16] D. Yang, J. Liu, Y. Zhang, and S. Zhang, "Optimal surface profile design of deployable mesh reflectors via a force density strategy," *Acta Astronautica*, vol. 130, pp. 137–146, 2017.

[17] S. Morterolle, B. Maurin, J. Quirant, and C. Dupuy, "Numerical form-finding of geotensoid tension truss for mesh reflector," *Acta Astronautica*, vol. 76, pp. 154–163, 2012.

[18] S. C. Yuan and B. E. Yang, "The fixed nodal position method for form finding of high-precision lightweight truss structures," *International Journal of Solids and Structures*, vol. 161, pp. 82–95, 2019.

[19] D. Yang, Y. Zhang, P. Li, and J. Du, "Numerical form-finding method for large mesh reflectors with elastic rim trusses," *Acta Astronautica*, vol. 147, pp. 241–250, 2018.

[20] R. Nie, B. He, L. Zhang, and Y. Fang, "Deployment analysis for space cable net structures with varying topologies and parameters," *Aerospace Science and Technology*, vol. 68, pp. 1–10, 2017.

[21] R. Nie, B. He, D. H. Hodges, and X. Ma, "Form finding and design optimization of cable network structures with flexible frames," *Computers & Structures*, vol. 220, pp. 81–91, 2019.

[22] R. Nie, B. He, D. H. Hodge, and X. Ma, "Integrated form finding method for mesh reflector antennas considering the flexible truss and hinges," *Aerospace Science and Technology*, vol. 84, pp. 926–937, 2019.

[23] R. Nie, B. He, S. Yan, and X. Ma, "Optimization design method for the cable network of mesh reflector antennas considering space thermal effects," *Aerospace Science and Technology*, vol. 94, article ???, 2019.

[24] H. Shi, S. Yuan, and B. Yang, "New methodology of surface mesh geometry design for deployable mesh reflectors," *Journal of Spacecraft and Rockets*, vol. 55, no. 2, pp. 266–281, 2018.

[25] M. Tabata and M. C. Natori, "Active shape control of a deployable space antenna reflector," *Journal of Intelligent Material Systems and Structures*, vol. 7, no. 2, pp. 235–240, 1996.

[26] A. Meguro, S. Harada, and M. Watanabe, "Key technologies for high-accuracy large mesh antenna reflectors," *Acta Astronautica*, vol. 53, no. 11, pp. 899–908, 2003.

[27] H. Tanaka, N. Shimozono, and M. C. Natori, "A design method for cable network structures considering the flexibility of supporting structures," *Transactions of the Japan Society for Aeronautical and Space Sciences*, vol. 50, no. 170, pp. 267–273, 2008.

[28] H. Tanaka and M. C. Natori, "Shape control of cable-network structures based on concept of self-equilibrated stresses," *JSME International Journal Series C Mechanical Systems, Machine Elements and Manufacturing*, vol. 49, no. 4, pp. 1067–1072, 2006.

[29] H. Tanaka, "Design optimization studies for large-scale contoured beam deployable satellite antennas," *Acta Astronautica*, vol. 58, no. 9, pp. 443–451, 2006.

[30] A. Meguro, "Development of a 15m class modular mesh deployable antenna," in *48th International Astronautical Congress*, Turin, Italy, 1997.

[31] M. Thomson, "Astromesh deployable reflectors for ku and ka band commercial satellites," in *20th AIAA International Communication Satellite Systems Conference and Exhibit*, Montreal, Quebec, Canada, 2002.

[32] M. Tabata, M. C. Natori, T. Tashima, and T. Inoue, "Adjustment procedure of a high precision deployable mesh antenna for MUSES-B spacecraft," *Journal of Intelligent Material Systems and Structures*, vol. 8, no. 9, pp. 801–809, 1997.

[33] M. C. Natori, T. Takano, and T. Noda, "Ground adjustment procedure of a deployable high accuracy mesh antenna for space VLBI mission," in *39th AIAA/ASME/ASCE/AHS/ASC Structures, Structural Dynamics, and Materials Conference and Exhibit*, Long Beach,CA,U.S.A., 1998.

[34] H. Tanaka, "Study on a calibration method for shape control parameters of a self-sensing reflector antenna equipped with surface adjustment mechanisms," *Transactions of the Japan Society for Aeronautical and Space Sciences*, vol. 57, no. 2, pp. 86–92, 2014.

[35] G. L. Su, Y. Li, Y. S. Fan, H. Li, and X. Ma, "Prestress optimal design of deployable antenna considering the effect of gravity," in *20th International Symposium on Distributed Computing and Applications for Business, Engineering and Science*, Nanning, China, 2021.